Journal of Medicinal Chemistry

Article

pubs.acs.org/jmc

Azaindoles: Noncovalent DprE1 Inhibitors from Scaffold Morphing Efforts, Kill *Mycobacterium tuberculosis* and Are Efficacious *in Vivo*

Pravin S. Shirude,*[,†,#] Radha Shandil,[§] Claire Sadler,[∥] Maruti Naik,[†] Vinayak Hosagrahara,[§] Shahul Hameed,[†] Vikas Shinde,[†] Chandramohan Bathula,[†] Vaishali Humnabadkar,[‡] Naveen Kumar,[§] Jitendar Reddy,[§] Vijender Panduga,[§] Sreevalli Sharma,[‡] Anisha Ambady,[‡] Naina Hegde,[‡] James Whiteaker,[⊥] Robert E. McLaughlin,[⊥] Humphrey Gardner,[⊥] Prashanti Madhavapeddi,[‡] Vasanthi Ramachandran,[‡] Parvinder Kaur,[‡] Ashwini Narayan,[‡] Supreeth Guptha,[‡] Disha Awasthy,[‡] Chandan Narayan,[‡] Jyothi Mahadevaswamy,[‡] KG Vishwas,[§] Vijaykamal Ahuja,[§] Abhishek Srivastava,[§] KR Prabhakar,[§] Sowmya Bharath,[§] Ramesh Kale,[†] Manjunatha Ramaiah,[†] Nilanjana Roy Choudhury,[†] Vasan K. Sambandamurthy,[‡] Suresh Solapure,[§] Pravin S. Iyer,[†] Shridhar Narayanan,[‡] and Monalisa Chatterji*[,‡,#]

[†]Department of Medicinal Chemistry, IMED Infection, AstraZeneca India, Bellary Road, Hebbal, Bangalore 560024, India

[‡]Department of Biosciences, IMED Infection, AstraZeneca, Bangalore 560024, India

[§]DMPK and Animal Sciences, IMED Infection, AstraZeneca, Bangalore 560024, India

[∥]Safety Assessment, IMED Infection, AstraZeneca, Alderly Park, Mereside, U.K.

[⊥]Translational Science, IMED Infection, AstraZeneca, Waltham, Massachusetts, United States

Supporting Information

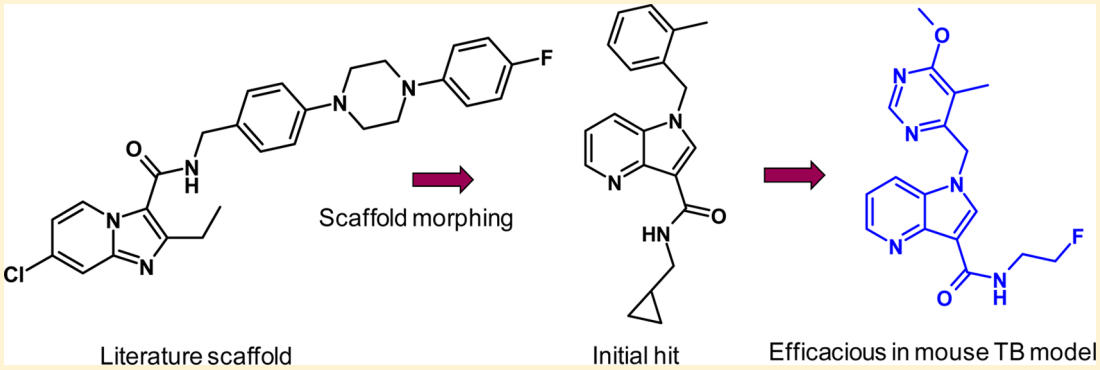

ABSTRACT: We report 1,4-azaindoles as a new inhibitor class that kills *Mycobacterium tuberculosis in vitro* and demonstrates efficacy in mouse tuberculosis models. The series emerged from scaffold morphing efforts and was demonstrated to noncovalently inhibit decaprenylphosphoryl-β-D-ribose2′-epimerase (DprE1). With "drug-like" properties and no expectation of pre-existing resistance in the clinic, this chemical class has the potential to be developed as a therapy for drug-sensitive and drug-resistant tuberculosis.

INTRODUCTION

Tuberculosis (TB) continues to cause considerable morbidity and mortality worldwide despite an effective and economical quadruple drug therapy regimen put in place 40 years ago.[1,2] However, long duration of therapy, associated toxicity, and emergence of multidrug-resistant tuberculosis (MDR-TB) has created an urgent need for new drugs. The U.S. Food and Drug Administration's accelerated approval of Janssen's Sirturo (bedaquiline) for MDR-TB ended a four-decade-long drought of a new TB drug with a novel mechanism of action.[3] However, the impact of Sirturo on the disease landscape and patient's lives needs to be evaluated in the context of associated safety risks and the burden of post marketing studies.[3]

Nitro-benzothiazinones (BTZs) are known inhibitors of decaprenylphosphoryl-β-D-ribose2′-epimerase (DprE1). DprE1 is involved in the conversion of decaprenylphosphoryl-β-D-ribose (DPR) to decaprenylphosphoryl-β-D-arabinofuranose (DPA), a precursor of mycobacterial cell wall arabinan.[4] This reaction is catalyzed by a heteromeric enzyme decaprenyl-phospho-ribose 2′-epimerase (DprE), via a sequential oxida-

Received: September 10, 2013

   dx.doi.org/10.1021/jm401382v | J. Med. Chem. XXXX, XXX, XXX−XXX

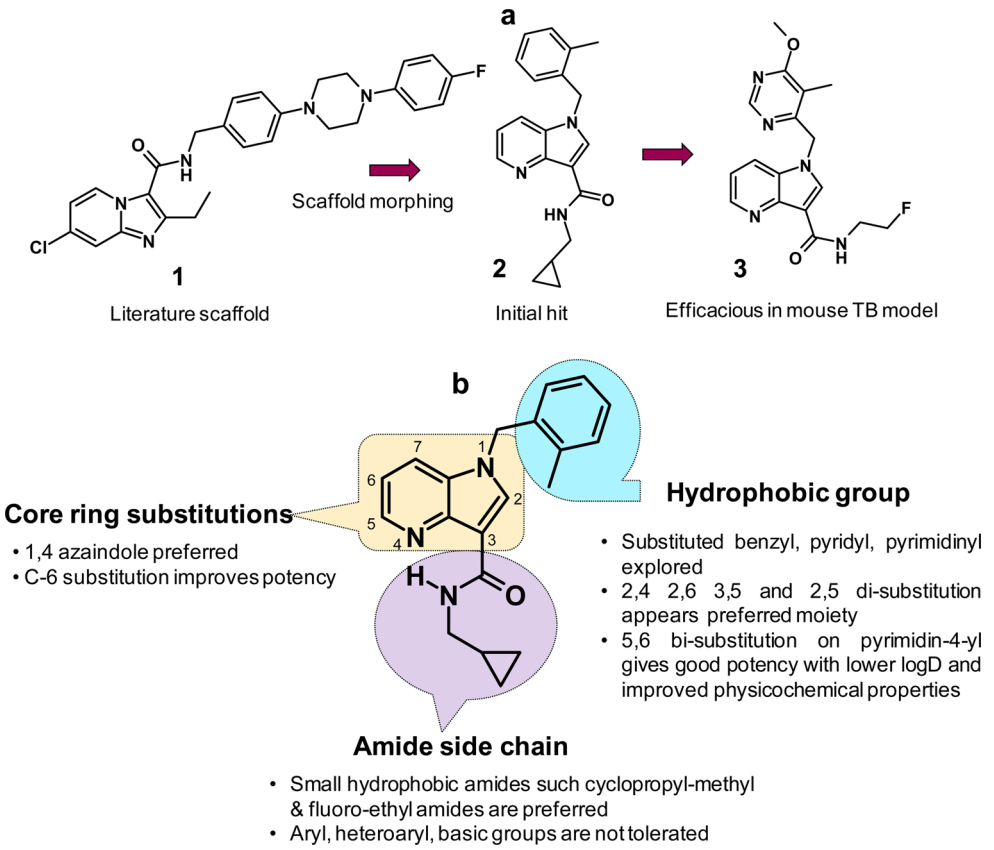

Figure 1. Identification of 1,4-azaindoles. (a) Scaffold morphing: **1**, imidazolopyridine; **2** 1,4-azaindole, initial hit; **3**, 1,4-azaindole-optimized compound. (b) Structure−activity relationship for 1,4-azaindoles.

tion−reduction mechanism involving decaprenylphosphoryl-2-keto-β-D-*erythro*-pentofuranose, (DPX) as an intermediate. DprE1 is composed of two proteins encoded by the *dprE1* and *dprE2* genes, and the DprE1 enzyme is an FAD-containing oxidoreductase while DprE2 is an NADH-dependent reductase.[5,6]

The identification of BTZ043 as a covalent inhibitor of DprE1 with potent antimycobacterial activity confirms the validity of this target for discovery of novel TB drugs.[6] However, it remains to be understood whether noncovalent inhibition of DprE1 will lead to *in vivo* efficacy. Moreover, it also needs be tested if nanomolar-level cellular activity (observed for BTZ043) is required for DprE1 inhibitors to be efficacious *in vivo*. Understanding of the relationship between mode of inhibition of the target, its translation to cellular potency, and ultimately efficacy in animal models, will significantly influence future TB drug discovery efforts directed at this target. In this paper, we present a scaffold morphing approach that led to the identification of the "1,4-azaindole" scaffold as a novel bactericidal inhibitor class. The compounds in the series have drug like properties, are noncovalent inhibitors of DprE1, and demonstrate efficacy in mouse tuberculosis models. These key attributes highlight the potential of this series to be developed for the treatment of drug sensitive and drug resistant tuberculosis therapy.

RESULTS AND DISCUSSION

The 1,4-azaindoles described herein were identified from a scaffold morphing approach starting with a published anti-TB, non-DprE1 imidazo-pyridine scaffold.[7,8] The imidazo-pyridine compound **1** (Figure 1a) exhibited a potent minimal inhibitory concentration (MIC, 0.017 μM, Table 1) against *Mycobacterium tuberculosis* (Mtb) H37Rv but lacked an effective minimum bactericidal concentration (MBC, >200 μM), suggesting its static nature. The early scaffold-morphed hit **2** displayed a moderate MIC (6.25 μM) but also, encouragingly, moderate cidality (MBC, 12.5 μM) (Figure 1a, Table 1). We have established a MIC-based structure−activity relationship (SAR) against Mtb. Three points of diversification were identified for the 1,4-azaindoles, namely the amide side chain, a hydrophobic group, and core ring substitutions (Figure 1b). The secondary amide (referred to as the amide side chain in Figure 1b) is an essential group for maintaining potent MIC and that could be involved in either intramolecular hydrogen bonding with nitrogen (N4) of the azaindole ring or hydrogen bonding with the target enzyme (compound **2**−**9** vs compound **10**, Tables 1 and 2). Small hydrophobic or hydrophilic amides

Table 1. Microbiological Properties of Key Compounds[a]

no.	Mtb MIC (μM)	Mtb MBC (μM)	Mtb HBC (μM)	DprE1 IC_{50} (μM)	MMIC (μM)
1	0.017	>200	>100	>10	ND
2	6.25	12.5	>100	0.014	94
3	1.56−3.12	1.56−3.12	50	0.010−0.017	>100
4	0.39−1.56	0.78−1.56	>100	0.005−0.015	>100
5	<0.39	<0.39	100	0.003−0.015	>100
6	1.56−3.12	0.78−1.56	>100	0.010−0.03	>100

[a]ND: not determined.

dx.doi.org/10.1021/jm401382v | J. Med. Chem. XXXX, XXX, XXX−XXX

Table 2. Structure−Activity Relationship of 1,4-Azaindoles[a]

No	Structure	MIC (μM)	IC_{50} (μM)	No	Structure	MIC (μM)	IC_{50} (μM)
4	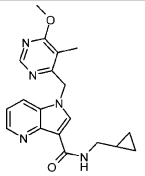	0.39	0.005	**14**	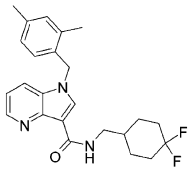	>200	7.9
5	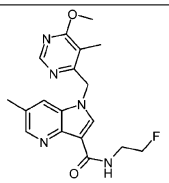	<0.39	0.003	**15**	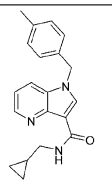	13.2	0.021
6	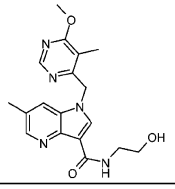	1.56	0.010	**16**	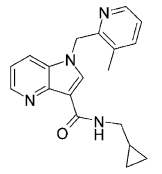	27	0.083
7	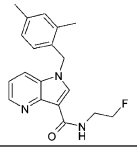	1.56-3.12	0.010	**17**	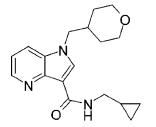	>100	2.5
8	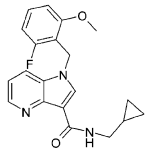	1.56-3.12	0.006	**18**	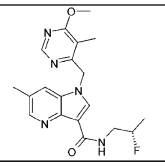	0.156	0.014
9	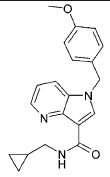	6.25	0.007	**19**	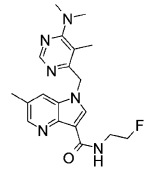	0.78	0.037
10	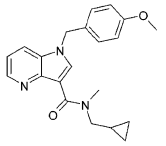	> 200	>10	**20**	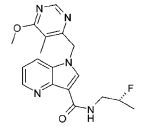	0.78	ND
11	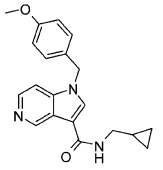	> 200	1	**21**	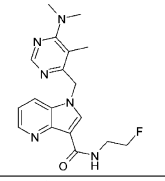	6.25	0.020
12	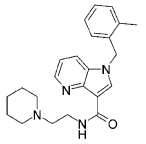	> 200	>10	**22**	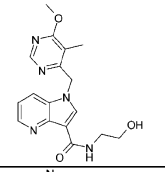	14	0.090
13	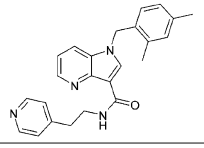	> 200	5.5	**23**	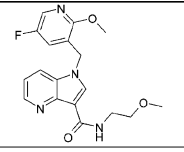	0.78-3.12	0.004

[a]ND = not determined.

dx.doi.org/10.1021/jm401382v | J. Med. Chem. XXXX, XXX, XXX−XXX

Table 3. 1,4-Azaindoles: DMPK and Safety Properties[a]

compound	2	3	4	5	6
log *D*	>4.5	2.1	3.0	2.6	1.8
solubility (μM)	3[b]	8[b]	5[b]	4[b]	124
human CL_{pred} microsomes (% LBF)	10	6	13	10	13
human CL_{pred} hepatocytes (% LBF)	ND	7	6	9	15
rat CL_{pred} hepatocytes (% LBF)	35	20	18	26	24
dog CL_{pred} hepatocytes (% LBF)	ND	25	20	26	16
human PPB (% free)	<1	9.8	5	5	22
Caco-2 A−B/B−A (1×10^{-6}·cm/s)	ND	25/17	38/24	33/17	11/30
CYP[c] inhibition (μM)	ND	>50	>50	>50	>50
hERG (μM)	28	>33	>33	>33	>33
secondary pharmacology hits IC_{50} (μM)	ND	no significant hits[d]			

[a]ND: not determined. [b]Kinetic solubility in test media >100 μM. [c]CYP1A2, CYP2C9, CYP2C19, CYP2D6, CYP3A4. [d]Panel of 24 high severity targets (binding and functional data): IC_{50} >100 μM or >30 μM.

such as methyl cyclopropyl, fluoro-ethyl, and hydroxy ethyl amides are preferred for cellular potency (compounds **2**−**5** and **7**−**8** vs compound **12**−**14**, Tables 1 and 2).

Additionally, the amide side chain influences physicochemical properties and *in vitro* safety parameters (Table 3). The hydrophobic group tolerates various disubstituted benzyl and disubstituted heteroaryl-methyl groups; however, monosubstituted benzyl groups are less favored (compound **2**, **9**, and **15**−**16** vs compound **3**−**8**, Tables 1 and 2). These groups are also critical to modulate MIC, physicochemical, and *in vitro* safety properties (Tables 1−3). Addition of a methyl group at the C-6 position of the 1,4-azaindole improved cellular potency (compound **3** and **20**−**22** vs compound **5**−**6** and **18**−**19**, Tables 1 and 2). Thus, the scaffold has multiple diversity points to build in required properties. Overall, the series contains compounds with submicromolar MICs and MBCs (Table 1, MBC/MIC ratio 1−2).

The 1,4-azaindole series, although cidal for Mtb and *Mycobacterium smegmatis* (Msm), did not show activity against a broad panel of Gram negative and Gram positive pathogens, thus suggesting an excellent target pathogen specificity (Supporting Information Table S1). Compounds in the series retained their MIC against a panel of drug sensitive and single-drug resistant clinical isolates of Mtb (Supporting Information Table S2), establishing a case for their potential use against drug sensitive and MDR TB infections. Compounds **3** and **4** exhibited time-dependent kill kinetics against replicating Mtb, with ∼4 $\log_{10}$ reductions in colony forming units (CFU) by day 10 at a concentration of 1−4 fold MIC (Figure 2a,b). Compounds **3** and **4** were also active against intracellular Mtb in THP-1 cells, with ∼1−2 $\log_{10}$ reduction in CFU at concentrations 1−4-fold of MIC (Supporting Information Figure S1). In addition to potent activity on replicating bacteria, compound **3** showed weak to moderate activity against nonreplicating Mtb grown under hypoxic conditions (∼1.5 $\log_{10}$ reduction in CFU at 30 fold of MIC; HBC)[9] (Table 1). Compounds **2**−**6** were found to be noncytotoxic against a human lung adenocarcinoma epithelial cell line (A549) following 72 h of compound exposure (MMIC >100 μM, Table 1).

Spontaneous resistant mutants to compounds **7** and **8** arose at a frequency of 2.9×10^{-9} at eight times MIC concentration (Supporting Information Table S3). Mutant strains showed about 10−100-fold upward shift in MIC with respect to wild-type H37Rv strain (Supporting Information Table S3). Whole genome sequencing of the resistant Mtb mutants revealed a single nucleotide change in DprE1 (Rv3790), resulting in an amino acid substitution (Tyr → His) at position 314. No significant secondary targets were observed from the whole genome sequencing analysis of multiple resistant strains, while compounds in the 1,4-azaindole series showed resistance to Y314H mutant strain (Table 4) and cross-resistance was not observed for series of reference drugs including BTZ043 (Supporting Information Table S4). The cysteine-387 DprE1 mutants (Cys → Ser, Cys → Gly) that impart resistance to BTZ043[6] did not show cross resistance to 1,4-azaindoles (compounds **3**−**6**, Table 4). Target specificity was further confirmed by the reduced sensitivity of a DprE1 overexpression strain (Mtb DprE1 OE) to compounds **3**−**6** similar to BTZ043 (Table 4). Additionally, the compounds in the series show potent inhibition of DprE1 enzyme,[10] confirming its target (Table 4). About a thousand-fold shift in IC_{50} was observed for purified Msm Y321H (Y314H in Mtb) mutant enzyme compared to wild-type enzyme, whereas the IC_{50} for Cys394G (Cys 387 in Mtb) mutants were comparable to that of wild-type. The inhibition of mutant enzymes compared to the wild-type correspond very well with the cellular potency, thus strengthening the understanding of DprE1 being the target for this series (Table 4). Mass spectrometric analysis of Msm DprE1 treated with compound **22** and **23** did not reveal a covalent adduct, confirming a noncovalent mode of inhibition. As previously reported,[6] BTZ043 showed a covalent adduct under the same experimental conditions (Supporting Information Figure S2). This result confirms a different binding mode for the 1,4-azaindoles described here in comparison to BTZ043.

Compounds in the series were profiled for *in vitro* drug metabolism and pharmacokinetic (DMPK) properties as depicted in Table 3. The dried DMSO solubility for compounds **3**−**5** was lower than compound **6**; the improved solubility can be attributed to hydroxyethyl amide side chain. The human plasma protein binding (PPB, % free) values for compounds **3**−**6** were between 5% and 22%. On the basis of *in vitro* intrinsic clearance (Cl_{int}) using human microsomes, human hepatocytes, rat hepatocytes, and dog hepatocytes, the predicted *in vivo* clearance (CL) for compounds **3**−**6** ranged between 6 and 26% of liver blood flow (% LBF). In contrast, the *in vitro* intrinsic clearance was higher from mouse microsomes (Supporting Information Table S5), suggesting species specific clearance mechanisms. The permeability as measured by Caco2 assay suggested that these compounds are highly permeable with no significant efflux activity. The compounds in the series did not show inhibition of cytochrome

dx.doi.org/10.1021/jm401382v | J. Med. Chem. XXXX, XXX, XXX−XXX

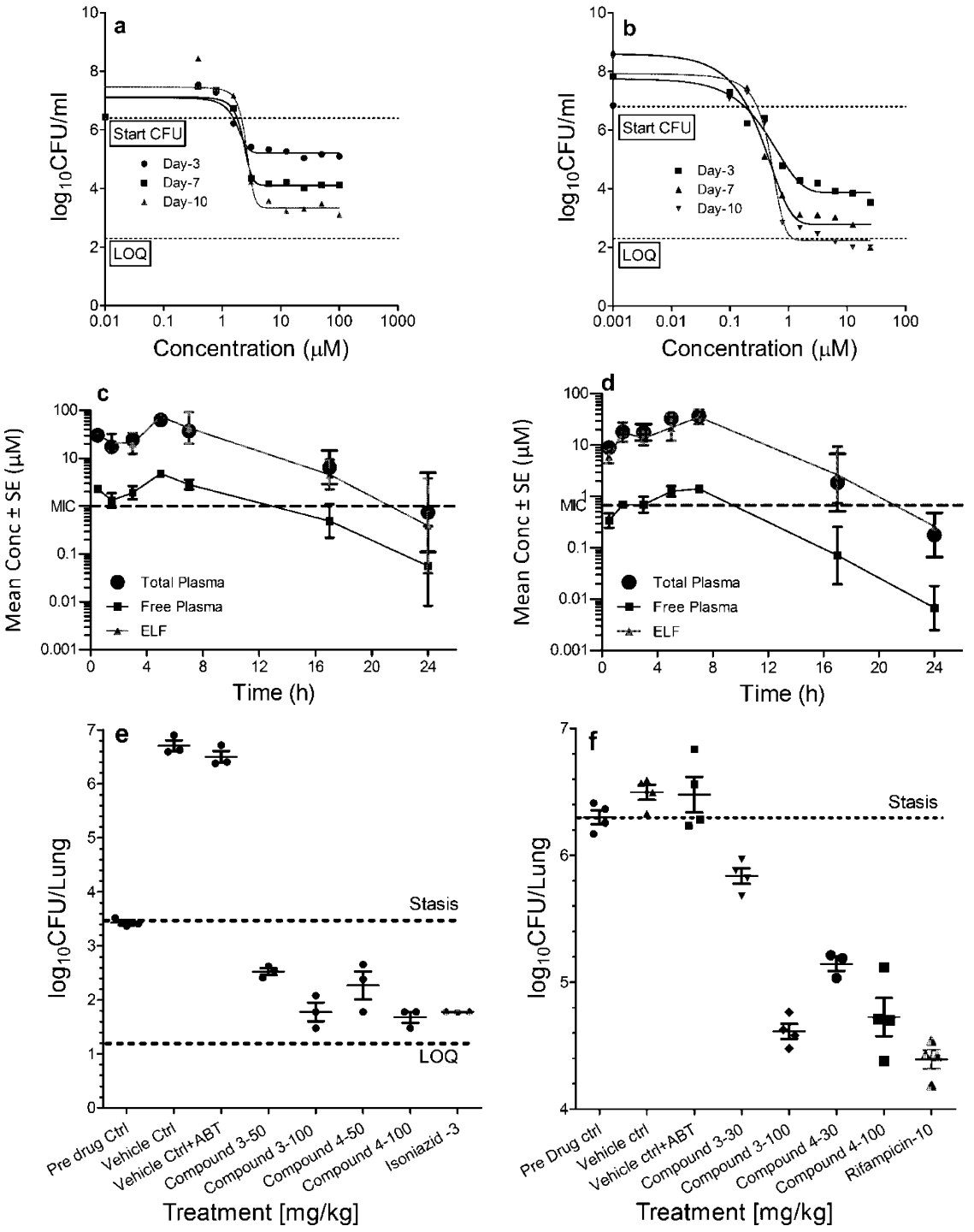

Figure 2. 1,4-Azaindoles: *in vitro* cell cidality, ELF PK, and *in vivo* efficacy. (a) Kinetic of cell cidality for compound **3**. (b) Kinetic of cell cidality for compound **4**. (c) ELF PK of compound **3** in healthy mice at 100 mg/kg. (d) ELF PK of compound **4** in healthy mice at 100 mg/kg. (e) Efficacy in acute TB infection model. (f) Efficacy in chronic TB infection model.

Table 4. Cross-Resistance of 1,4-Azaindoles

	Mtb MIC (μM)					Msm DprE1 purified enzyme IC_{50} (μM)		
no.	H37Rv	DprE1 OE	DprE1 C387S	DprE1 C387G	DprE1 Y314H	DprE1 WT	DprE1 C394G	DprE1 Y321H
3	3.12	50	3.12	0.78	>100	0.017	0.015	>10
4	0.39	25	0.39	0.39	>200	0.006	ND	2.6
5	0.39	6.25	0.39	0.39	>200	0.017	0.007	>10
6	1.56	100	0.39	0.78	>200	0.01	0.01	>10

dx.doi.org/10.1021/jm401382v | J. Med. Chem. XXXX, XXX, XXX−XXX

P450 (CYP) enzymes at 50 μM (Table 3), suggesting their low potential for drug−drug interactions. *In vitro* safety profiling of compounds **3**−**6** against a panel of human targets and cardiac channels has indicated no major safety liabilities associated with this series (Table 3).

On the basis of *in vitro* properties, compounds **3**−**6** were administered to mice and rats to assess their *in vivo* PK parameters. Exposure in mice was measured in the presence of 1-aminobenzotriazole (ABT), a pan-inhibitor of CYP isoforms used to block mouse specific clearance. Good oral exposure was observed for compounds **3**−**6** in both rats and mice (Supporting Information Figure S3, Supporting Information Table S6). In rats, good correlation was observed between *in vitro* and *in vivo* clearance (Supporting Information Table S6). The *in vivo* efficacy of two representative compounds (**3** and **4**) was assessed in BALB/c mice in "acute" and "chronic" TB infection models.[11,12] In the acute infection model, treatment was initiated 3 days postinfection, whereas treatment was started on day 28 in the chronic infection model. After four weeks of treatment with compound **3** and **4**, the bacterial burden in the lungs was reduced by >1.5 $\log_{10}$ CFU and statistically significant dose dependent efficacy was observed in both the models (Figure 2e,f). The observed moderate hypoxia activity for compound **3** does not appear to contribute significantly to the efficacy results observed in mouse. The oral exposure of compounds **3** and **4**, assessed from infected animals showed AUCs ranging from 200 to 700 μM·h and free plasma concentrations were maintained above the MIC for 10−24 h (%fT > MIC of 25−100), resulting in efficacy in the acute and chronic TB infection models (Supporting Information Figure S4, Supporting Information Table S7). Interestingly, the concentration of compounds **3** and **4** measured in lung epithelial lining fluid of healthy mice (ELF PK) compared to the total plasma concentration for both the compounds (Figure 2C, Supporting Information Table S8), demonstrating significant distribution to the target site. Thus, a good correlation was observed between plasma and ELF levels and the pharmacodynamic effect. No adverse events in the form of body weight loss, organ weight loss, or gross pathology were observed following 4 weeks of repeated dosing in the efficacy studies.

CONCLUSIONS

In summary, we have employed a scaffold morphing approach to discover a novel series of 1,4-azaindoles with antituberculosis activity. We have established that this novel inhibitor class exhibits cellular activity via a noncovalent inhibition of DprE1. This mode of inhibition (MOI) and level of cellular activity translates and are sufficient to show efficacy in a relevant TB mouse model. Recent work from Wang *et al.*, identified TCA1, through cell-based phenotypic screen, which has two cellular targets, DprE1 and MoeW enzymes, and has been found to be efficacious in mouse TB models.[13] On the basis of *in vivo* efficacy, drug like properties and absence of *in vitro* safety liabilities, the "1,4-azaindole" series warrants further investigation for *in vivo* safety. We believe this series has the potential to deliver a candidate drug for TB.

EXPERIMENTAL SECTION

All anhydrous solvents, reagent grade solvents for chromatography, and starting materials were purchased from either Sigma Aldrich Chemical Co. or Fisher Scientific. Water was distilled and purified through a Milli-Q water system (Millipore Corp., Bedford, MA). General methods of purification of compounds involved the use of silica cartridges purchased from Grace Purification systems. The reactions were monitored by TLC on precoated Merck 60 F254 silica gel plates and visualized using UV light (254 nm). All compounds were analyzed for purity by HPLC and characterized by ^{1}H NMR using Bruker 300 MHz NMR and/or Bruker 400 MHz NMR spectrometers. Chemical shifts are reported in ppm (δ) relative to the residual solvent peak in the corresponding spectra; chloroform δ 7.26, methanol δ 3.31, DMSO δ 2.5, and coupling constants (J) are reported in hertz (Hz) (where s = singlet, bs = broad singlet, d = doublet, dd = double doublet, bd = broad doublet, ddd = double doublet of doublet, t = triplet, tt = triple triplet, q = quartet, m = multiplet) and analyzed using ACD NMR data processing software. Mass spectra values are reported as m/z. All reactions were conducted under nitrogen unless otherwise noted. Solvents were removed in vacuo on a rotary evaporator. All final compounds for biological testing were purified by reverse phase HPLC with >95% purity (Shimadzu HPLC instrument with a Hamilton reversed phase column (HxSil, C18, 3 μm, 2.1 mm × 50 mm (H2)). Eluent A, 5% CH_3CN in H_2O; eluent B, 90% CH_3CN in H_2O. A flow rate of 0.2 mL/min was used with UV detection at 254 and 214 nm]

Abbreviations: NMP = *N*-methyl pyrrolidine HCl = hydrochloric acid DMF = *N*,*N*-dimethylformamide NaH = sodium hydride. EI = electrospray ionization HRMS = high resolution mass spectrometry.

***N*-(Cyclopropylmethyl)-1-(2-methylbenzyl)-1*H*-pyrrolo[3,2-*b*]pyridine-3-carboxamide (2).** 1-(2-Methylbenzyl)-1*H*-pyrrolo-[3,2-*b*]pyridine-3-carboxylic acid (120 mg, 0.45 mmol) was placed in a 50 mL single-necked flask equipped with a reflux condenser connected to a nitrogen source. Thionyl chloride (5 mL, 0.45 mmol) was added, and the mixture was heated at reflux overnight. The excess thionyl chloride was evaporated to dryness (residue 1). In another flask, cyclopropanemethylamine (0.195 mL, 2.25 mmol) was dissolved in dichloromethane (10 mL), and triethylamine (0.312 mL, 2.25 mmol) was added. The mixture was stirred at RT for 10 min, then added slowly to residue 1 to give a suspension which was stirred at RT for 1 h. After completion of the reaction, DCM was added and the mixture was washed with water and brine solution. The DCM layer was dried over sodium sulfate and evaporated, and the residue was purified by column using methanol/DCM (yield 53%). ES + MS m/z: 320 (M + 1). ^{1}H NMR (300 MHz, DMSO-d_6) δ ppm 0.21−0.34 (m, 2 H) 0.41−0.57 (m, 2 H) 0.98−1.17 (m, 1 H) 2.28 (s, 3 H) 3.28 (t, J = 6.22 Hz, 2 H) 5.55 (s, 2 H) 6.70 (d, J = 7.35 Hz, 1 H) 7.05−7.17 (m, 1 H) 7.17−7.35 (m, 3 H) 7.99 (d, J = 8.29 Hz, 1 H) 8.14 (s, 1 H) 8.53 (d, J = 4.52 Hz, 1 H) 8.82 (t, J = 5.56 Hz, 1 H). ^{13}C NMR (400 MHz, DMSO-d_6) δ ppm 162.6, 143.6, 142.4, 135.8, 135.7, 134.8, 130.4, 129.6, 127.8, 126.9, 126.2, 119.3, 117.3, 110, 48, 42.4, 18.6, 11.2, 3.2.

***N*-(2-Fluoroethyl)-1-((6-methoxy-5-methylpyrimidin-4-yl)-methyl)-1*H*-pyrrolo[3,2-*b*]pyridine-3-carboxamide (3).** 1-((6-Methoxy-5-methylpyrimidin-4-yl)methyl)-1*H*-pyrrolo[3,2-*b*]pyridine-3-carboxylic acid (250 mg, 0.84 mmol) was placed in a 100 mL single-necked flask equipped with an air condenser connected to a nitrogen source. DCM (20 mL) was added, followed bytriethyl amine (1.162 mL, 8.38 mmol) to give a clear solution. 1-Propanephosphonic acid cyclic anhydride (1.497 mL, 2.51 mmol) was added, followed by 2-fluoroethanamine hydrochloride (83 mg, 0.84 mmol). The reaction mixture was stirred at RT overnight. After completion of the reaction, DCM and water was added. The layers were separated, and the DCM layer was washed with brine, dried over sodium sulfate and evaporated, and the residue was purified by column using methanol/DCM (yield 52%). ES + MS m/z: 344 (M + 1). ^{1}H NMR (300 MHz, DMSO-d_6) δ ppm 2.25 (s, 20 H) 3.67 (d, J = 5.46 Hz, 7 H) 3.77 (d, J = 5.46 Hz, 7 H) 4.50 (t, J = 4.90 Hz, 7 H) 4.66 (t, J = 4.99 Hz, 7 H) 5.69 (s, 13 H) 7.26 (dd, J = 8.29, 4.71 Hz, 7 H) 7.94 (d, J = 8.48 Hz, 7 H) 8.28 (s, 7 H) 8.41 (s, 6 H) 8.49 (d, J = 4.52 Hz, 7 H) 8.95 (t, J = 5.84 Hz, 7 H). ^{13}C NMR (400 MHz, DMSO-d_6) δ ppm 167.2, 163, 161.2, 155, 143.3, 142.4, 137.1, 130.2, 119.4, 117.2, 114.6, 109.4, 83.8, 82.2, 54.1, 48.1, 38.6, 9.4.

***N*-(Cyclopropylmethyl)-1-((6-methoxy-5-methylpyrimidin-4-yl)methyl)-1*H*-pyrrolo[3,2-*b*]pyridine-3-carboxamide (4).** 1-((6-Methoxy-5-methylpyrimidin-4-yl)methyl)-1*H*-pyrrolo[3,2-*b*]pyridine-

dx.doi.org/10.1021/jm401382v | J. Med. Chem. XXXX, XXX, XXX−XXX

3-carboxylic acid (200 mg, 0.67 mmol) was taken in DCM (10 mL). 1-Propanephosphonic acid cyclic anhydride (427 mg, 1.34 mmol) was added, followed by the addition of triethyl amine (339 mg, 3.35 mmol) and cyclopropylmethanamine (95 mg, 1.34 mmol). The reaction mass was stirred at RT for overnight. After the completion of the reaction, water was added and extracted with DCM. The organic layer was washed with water and brine slution. The organic layer was separated and dried over sodium sulfate. The organic layer was evaporated to get the residue, which was purified by column chromatography to get the pure compound (yield 74%). ES + MS *m/z*: 352.38 (M + 1). ^{1}H NMR (300 MHz, DMSO-d_6) δ ppm 0.02 (q, J = 4.58 Hz, 2 H) 0.18−0.31 (m, 2 H) 0.83 (t, J = 6.88 Hz, 1 H) 2.00 (s, 3 H) 2.98−3.11 (m, 3 H) 3.69 (s, 3 H) 5.43 (s, 2 H) 7.00 (dd, J = 8.29, 4.71 Hz, 1 H) 7.68 (dd, J = 8.29, 1.13 Hz, 1 H) 7.98 (s, 1 H) 8.17 (s, 1 H) 8.24 (dd, J = 4.71, 1.13 Hz, 1 H) 8.55 (t, J = 5.75 Hz, 1 H). ^{13}C NMR (400 MHz, DMSO-d_6) δ ppm 167.2, 162.7, 161.2, 154.9, 143.3, 142.5, 136.9, 130.2, 119.3, 117.1, 114.6, 109.8, 54.1, 48, 42.4, 11.2, 9.4, 3.1.

***N*-(2-Fluoroethyl)-1-((6-methoxy-5-methylpyrimidin-4-yl)-methyl)-6-methyl-1*H*-pyrrolo[3,2-*b*]pyridine-3-carboxamide (5).** 1-((6-Methoxy-5-methylpyrimidin-4-yl)methyl)-6-methyl-1*H*-pyrrolo[3,2-*b*]pyridine-3-carboxylic acid (0.190 g, 0.61 mmol), 2-fluoroethanamine (0.077 g, 1.22 mmol), and TEA (0.254 mL, 1.83 mmol) was added in DCM. After 3 min, 1-propanephosphonic acid cyclic anhydride (0.484 g, 1.52 mmol) was added. The resulting reaction mixture was stirred at rt for 50 min. The reaction was diluted with DCM and water. The DCM layer was extracted and washed with brine and dried over sodium sulfate and concentrated. Purification was performed on Waters RP system to get product *N*-(2-fluoroethyl)-1-((6-methoxy-5-methylpyrimidin-4-yl)methyl)-6-methyl-1*H*-pyrrolo-[3,2-*b*]pyridine-3-carboxamide (0.090 g, 41.4%). ES + MS *m/z*: 358.36. ^{1}H NMR (300 MHz, DMSO-d_6) δ ppm 2.17−2.30 (3, 3 H) 2.40 (s, 3 H) 3.59−3.73 (m, 1 H) 3.73−3.83 (m, 1 H) 3.94 (s, 3 H) 4.50 (t, J = 4.99 Hz, 1 H) 4.66 (t, J = 4.99 Hz, 1 H) 5.64 (s, 2 H) 7.76 (s, 1 H) 8.15 (s, 1 H) 8.35 (s, 1 H) 8.42 (s, 1 H) 8.87 (t, J = 5.84 Hz, 1 H). ^{13}C NMR (400 MHz, DMSO-d_6) δ ppm 167.1, 163.1, 161.3, 155, 144.4, 140.6, 136.4, 130.3, 126.6, 119, 114.5, 109.3, 83.8, 82.2, 54.1, 47.9, 38.6, 18.3, 9.4.

***N*-(2-Hydroxyethyl)-1-((6-methoxy-5-methylpyrimidin-4-yl)-methyl)-6-methyl-1*H*-pyrrolo[3,2-*b*]pyridine-3-carboxamide (6).** 1-((6-Methoxy-5-methylpyrimidin-4-yl)methyl)-6-methyl-1*H*-pyrrolo[3,2-*b*]pyridine-3-carboxylic acid (75 mg, 0.24 mmol) was added to dichloromethane (10 mL) to give a suspension. Triethyl amine (66.9 mL, 0.48 mmol) was added, followed by 1-propane-phosphonic acid cyclic anhydride (286 mL, 0.48 mmol). The reaction mixture was stirred at RT for 5 min. Ethanol amine (29.0 mL, 0.48 mmol) was added, and the mixture was stirred at RT overnight. After completion of the reaction, the mixture was diluted with DCM and washed with water and brine. The DCM layer was dried over sodium sulfate and evaporated to give the crude product, which was purified by column chromatography using methanol/dichloromethane as eluent (yield 52.7%). ES + MS *m/z*: 356.4 (M + 1). ^{1}H NMR (300 MHz, DMSO-d_6) δ ppm 2.23 (s, 3 H) 2.39 (s, 3 H) 3.39−3.65 (m, 4 H) 3.93 (s, 3 H) 4.84 (t, J = 5.09 Hz, 1 H) 5.63 (s, 2 H) 7.74 (s, 1 H) 8.12 (s, 1 H) 8.33 (s, 1 H) 8.41 (s, 1 H) 8.80 (t, J = 5.65 Hz, 1 H). ^{13}C NMR (400 MHz, DMSO-d_6) δ ppm 167.1, 163, 161.3, 155, 144.3, 140.6, 136.2, 130.3, 126.4, 118.9, 114.5, 109.8, 60.3, 54.1, 47.9, 41, 18.3, 9.4.

■ ASSOCIATED CONTENT

Supporting Information

Details of the synthesis of all compounds and biological assays. This material is available free of charge via the Internet at http://pubs.acs.org.

■ AUTHOR INFORMATION

Corresponding Authors

*E-mail: pravin.shirude@astrazeneca.com. Phone: +91 080 23621212. Fax: +91 080 23621214.

*E-mail: monalisa.chatterji@astrazeneca.com.

Author Contributions

#P.S.S. and M.C. contributed equally.

Notes

The authors declare no competing financial interest.

■ ACKNOWLEDGMENTS

We thank the analytical support provided by S. Rudrapatna and the analytical team. Our sincere thanks to the PD Bangalore, CMG, Global DMPK, Safety, Biosciences (AZ Boston, USA), and Discovery Sciences (AZ, Alderly Park, UK) for technical support in various assays. We thank M. Panda for preliminary docking studies. We also thank Rajkumar and Subhash for animal welfare support. We sincerely thank G. Riccardi (University of Pavia) for providing the DprE1 expression plasmid. We thank Sudha R. for her contributions towards DprE1 overexpression strain. We acknowledge N. Dinesh and S. Ghorpade for scientific discussions. We also thank V. Balasubramanian, P. Warner, R. Tommasi, and M. Perros for their constant inspiration, support, and encouragement. This research was supported by the Global Alliance for Tuberculosis (GATB).

■ ABBREVIATIONS USED

TB, tuberculosis; Mtb, *Mycobacterium tuberculosis*; DprE1, decaprenylphosphoryl-β-D-ribose2′-epimerase 1; MDR-TB, multidrug-resistant tuberculosis; BTZs, nitro-benzothiazinones; DPR, decaprenylphosphoryl-β-D-ribose; DPA, decaprenylphosphoryl-β-D-arabinofuranose; DPX, decaprenylphosphoryl-2-keto-β-D-*erythro*-pentofuranose; MBC, minimum bactericidal concentration; MIC, minimum inhibitory concentration; SAR, structure−activity relationship; Msm, *Mycobacterium smegmatis*; DMPK, drug metabolism and pharmacokinetic; Cl_{int}, intrinsic clearance; PPB, plasma protein binding; CL, clearance; LBF, liver blood flow; CYP, cytochrome P450 enzymes

■ REFERENCES

(1) Raviglione, M.; Marais, B.; Floyd, K.; Lönnroth, K.; Getahun, H.; Migliori, G. B.; Harries, A. D.; Nunn, P.; Lienhardt, C.; Graham, S.; Chakaya, J.; Weyer, K.; Cole, S.; Kaufmann, S. H.; Zumla, A. Scaling up interventions to achieve global tuberculosis control: progress and new developments. *Lancet* **2012**, *379*, 1902−1913.

(2) *Global Tuberculosis Report*; World Health Organization: Geneva, 2012.

(3) Cohen, J. Approval of novel TB drug celebrated with restraint. *Science* **2013**, *339*, 130−131.

(4) Trefzer, C.; Rengifo-Gonzalez, M.; Hinner, M. J.; Schneider, P.; Makarov, V.; Cole, S. T.; Johnsson, K. Benzothiazinones: prodrugs that covalently modify the decaprenylphosphoryl-β-D-ribose 2′-epimerase DprE1 of *Mycobacterium tuberculosis*. *J. Am. Chem. Soc.* **2010**, *132*, 13663−13665.

(5) Mikušová, K.; Huang, H.; Yagi, T.; Holsters, M.; Vereecke, D.; D'Haeze, W.; Scherman, M. S.; Brennan, P. J.; McNeil, M. R.; Crick, D. C. Decaprenylphosphoryl arabinofuranose, the donor of the D-arabinofuranosyl residues of mycobacterial arabinan, is formed via a two step epimerization of decaprenylphosphoryl ribose. *J. Bacteriol.* **2005**, *187*, 8020−8025.

(6) Makarov, V.; Manina, G.; Mikušová, K.; Möllmann, U.; Ryabova, O.; Saint-Joanis, B.; Dhar, N.; Pasca, M. R.; Buroni, S.; Lucarelli, A. P.; Milano, A.; De Rossi, E.; Belanova, M.; Bobovska, A.; Dianiskova, P.; Kordulakova, J.; Sala, C.; Fullam, E.; Schneider, P.; McKinney, J. D.; Brodin, P.; Christophe, T.; Waddell, S.; Butcher, P.; Albrethsen, J.; Rosenkrands, I.; Brosch, R.; Nandi, V.; Bharath, S.; Gaonkar, S.; Shandil, R. K.; Balasubramanian, V.; Balganesh, T.; Tyagi, S.; Grosset, J.; Riccardi, G.; Cole, S. T. Benzothiazinones kill *Mycobacterium*

tuberculosis by blocking arabinan synthesis. *Science* **2009**, *324*, 801−804.
(7) No, Z.; Kim, J.; Brodin, P. B.; Seo, .M. J.; Kim, Y. M.; Cechetto, J.; Jeon, H.; Genovesio, A.; Lee, S.; Kang, S.; Ewann, F. A.; Nam, J. Y.; Christophe, T.; Fenistein, D. P.; Jamung, H.; Jiyeon, J. Anti-infective compounds. PCT publication no. WO 2011/113606 A1, 2011.
(8) No, Z.; Kim, J.; Brodin, P. B.; Seo, .M. J.; Park, E.; Cechetto, J.; Jeon, H.; Genovesio, A.; Lee, S.; Kang, S.; Ewann, F. A.; Nam, J. Y.; Fenistein, D. P.; Christophe, T.; Contreras Dominguez, M.; Kim, E.; Heo, J. Anti-infective pyrido(1,2-*a*)pyrimidines. PCT publication No. *WO 2011/085990 A1*, 2011.
(9) Wayne, L. G.; Hayes, L. G. An *in vitro* model for sequential study of shiftdown of *Mycobacterium tuberculosis* through two stages of nonreplicating persistence. *Infect. Immun.* **1996**, *64*, 2062−2069.
(10) Neres, J.; Pojer, F.; Molteni, E.; Chiarelli, L. R.; Dhar, N.; Boy-Röttger, S.; Buroni, S.; Fullam, E.; Degiacomi, G.; Lucarelli, A. P.; Read, R. J.; Zanoni, G.; Edmondson, D. E.; De Rossi, E.; Pasca, M. R.; McKinney, J. D.; Dyson, P. J.; Riccardi, G.; Mattevi, A.; Cole, S. T.; Binda, C. Structural Basis for Benzothiazinone-Mediated Killing of *Mycobacterium tuberculosis*. *Sci. Transl. Med.* **2012**, *4*, 150ra121.
(11) Jayaram, R.; Gaonkar, S.; Kaur, P.; Suresh, B. L.; Mahesh, B. N.; Jayashree, R.; Nandi, V.; Bharat, S.; Shandil, R. K.; Kantharaj, E.; Balasubramanian, V. Pharmacokinetics−Pharmacodynamics of Rifampin in an Aerosol Infection Model of Tuberculosis. *Antimicrob. Agents Chemother.* **2003**, *47*, 2118−2124.
(12) De Groote, M. A.; Gilliland, J. C.; Wells, C. L.; Brooks, E. J.; Woolhiser, L. K.; Gruppo, V.; Peloquin, C. A.; Orme, I. A.; Lenaerts, A. J. Comparative Studies Evaluating Mouse Models Used for Efficacy Testing of Experimental Drugs against *Mycobacterium tuberculosis*. *Antimicrob. Agents Chemother.* **2011**, *55*, 1237−1247.
(13) Wang, F.; Sambandan, D.; Halder, R.; Wang, J.; Batt, S. M.; Weinrick, B.; Ahmad, I.; Yang, P.; Zhang, Y.; Kim, J.; Hassani, M.; Huszar, S.; Trefzer, C.; Ma, Z.; Kaneko, T.; Mdluli, K. E.; Franzblau, S.; Chatterjee, A. K.; Johnson, K.; Mikusova, K.; Besra, G. S.; Fütterer, K.; Jacobs, W. R., Jr.; Schultz, P. G. Identification of a small molecule with activity against drug-resistant and persistent tuberculosis. *Proc. Natl. Acad. Sci.* **2013**, *110*, E2510−E2517.